ECE 445 Final Report,

Team 30: Transverse String Organ

By

Edward Perez

Kellen Sakaitani

Ash Huang

December 2025

Contents

1. Introduction

Electric guitar feedback is traditionally produced by amplifying the energy of the sound signal from the instrument so the signal can induce a sustained feedback loop in the guitar string. Products such as the EBow remove the inefficiency of energy transmission through sound by instead sending the amplified signal through magnetic driver coils directly into the string. Products such as this implement harmonic controls through analog filters in the signal chain, allowing the string to resonate in higher octaves.

Techniques such as this create a unique timbre from this instrument which can be finely controlled by the player and the electronics of the instrument. The timbre is restricted to a small number of notes (1-6 strings) at any given time and can only be utilized by musicians who are trained on guitar.

Our team bypasses these restrictions using a harp-like instrument with one feedback system per string. This instrument utilizes 12 strings representing the chromatic scale in the second musical octave and is controlled by a MIDI interface, allowing it to generalize to a broader range of musical controllers.

1.1 Requirements:

Notes should reach 63.2% max Vrms (Audible volume) within 0.2 seconds during activation, and should reach 36.8% max Vrms (Inaudible volume) within 0.2 seconds during dampening. This relates to the precision of timing at which we can play this instrument.

Small chords can be made: minimum 3 strings can ring out concurrently. These strings must be able to ring out for at least 20 seconds to be considered sustained indefinitely.

Harmonic control of each string is possible: The instrument can isolate strings at their fundamental frequency, and the 2nd & 4th harmonics (octave & 2 octaves). This will be measured using a waterfall diagram generated by an oscilloscope, ensuring that the active harmonic has a larger amplitude in fourier analysis than any other.

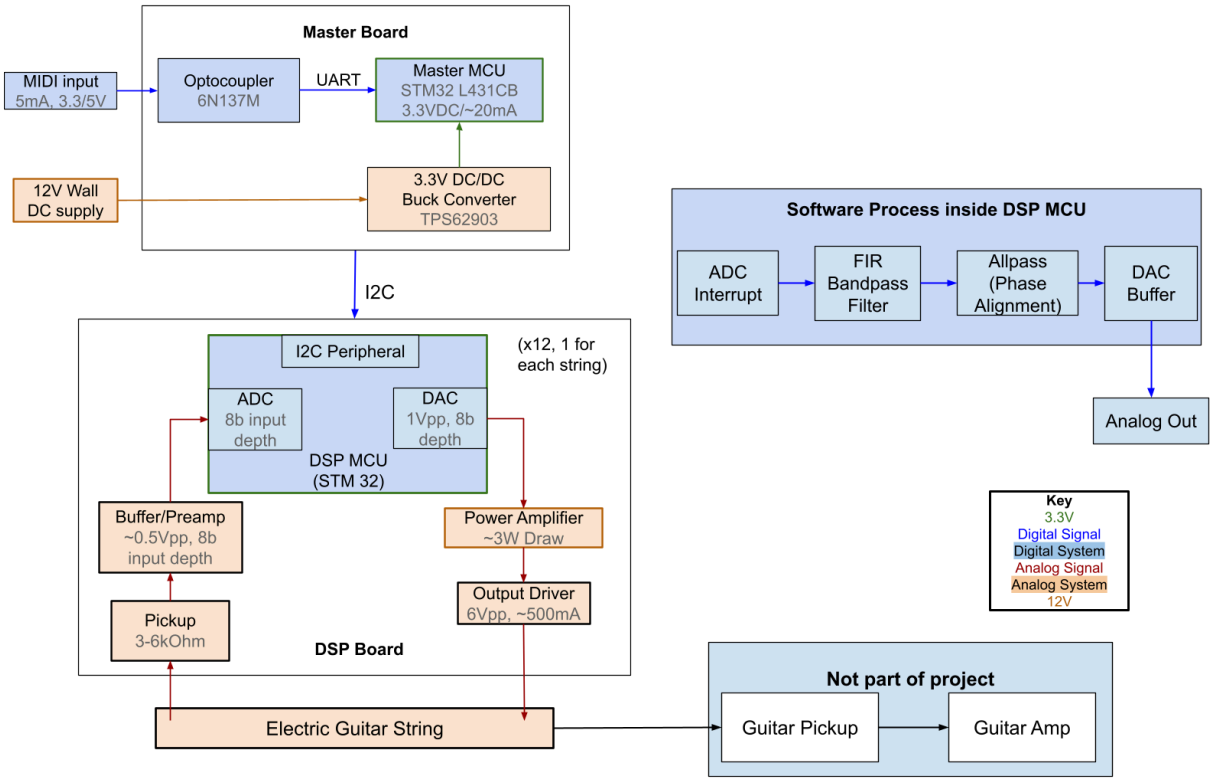

Figure 1.1: Block Digram

The instrument comprises two main systems: the Master Board and the individual DSP Feedback Systems.

The Master Board will act as the host of the system; it will listen to a MIDI signal through the UART peripheral of an STM microcontroller and translate specific MIDI commands to an I2C bus, where this system would act as the master. This board will also include a 3.3 V DC/DC regulator to power the MCUs of the other boards of the system.

On the slave side of the I2C bus will be several (1 per string) low-power, DSP microcontrollers. These microcontrollers will implement the synthesis and filtering that traditional sustain systems typically do using DSP rather than analog filters. This will allow us to perform extended functionality such as the automatic muting of notes, and more controlled harmonic filtering.

These DSPs will be paired with an electromagnetic pickup (similar to that of an electric guitar) to sample a signal from the string as it vibrates, and an electromagnetic driver which will receive an amplified & filtered version of the original signal in order to induce feedback into the string. An alternative approach for generating a signal would be to synthesize a signal for the driver to use. Each electromagnetic driver will be powered by a discrete class AB amplifier. The entire system can be powered by an off the shelf 12 V DC power supply.

2. Design

2.1 Design procedure

Master Board

The Master board utilizes an optocoupler, a master MCU, and a 3.3 V DC/DC converter, and is used to bridge the external MIDI controller to the slave boards connected over I2C.

Optocoupler

The optocoupler is used for reference isolation for the MIDI controller port. This is a standard circuit design for a MIDI receiver and requires minor peripheral circuitry to perform tasks such as ESD protection and signal biasing.

Master MCU

We selected a low power MCU capable of basic communications, and utilized the same MCU as the DSP boards, as the master MCU has a lower bandwidth requirement than the DSP boards. Utilizing the same MCU reduced cost by allowing more of the same component to be ordered in bulk. PCB ordering and assembly was streamlined due to our choice for each board layout to be identical. This meant components were selectively populated to differentiate between the two boards while the underlying PCB was identical between the master and slave boards. MCU selection was primarily constrained by the requirements of the DSP board; it will be discussed further in the DSP section.

We implemented a MIDI-controlled parsing system that routes musical control data from a MIDI controller to multiple DSP slaves through the master board. The system includes a master STM32 microcontroller and up to twelve slave STM32 microcontrollers connected through an I²C bus. Each slave was designed to control a single string which would support 3 notes each in the final instrument implementation. The master receives MIDI data from an external controller using a UART peripheral which is tuned to the standard MIDI baud rate of 31,250. It processes incoming MIDI data streams to identify Note On and Note Off messages, as well as valid note numbers before sending the corresponding control packets to slave devices over I²C. This process is proven to be low-latency with the use of interrupt driven design and a buffering system to be sure as few messages are dropped as possible.

Some design considerations included the handling of continuous MIDI streams accurately without data loss, ensuring non-blocking communication between devices, maintaining UART to I²C data flow at low latency, and allowing for scalability to multiple addressable slaves.

Several implementation strategies were tried and tested for the master board subsystem. While developing MIDI input support, a polling-based UART interface was initially considered but ultimately rejected due to the risk of missed bytes during high-traffic MIDI streams which had been observed during testing. An interrupt-driven UART configuration was then selected to

ensure that each received byte was processed immediately, minimizing the chance of a missed command.

MIDI message parsing was implemented using a finite-state machine rather than fixed-length message parsing. This approach was chosen to accommodate the MIDI protocol's variable-length messages and to support the protocol's running-status feature. The finite-state machine distinguishes between status and data bytes based on the most significant bit and maintains message context by storing completed messages in a message packet which can be stored inside a buffer.

For inter-device communication, I²C was selected over SPI to support multiple addressable slaves with minimal wiring complexity. To prevent I²C transmissions from blocking MIDI reception, I²C communication was implemented using non-blocking, fully interrupt-driven versions of HAL functions. A circular message buffer was introduced to isolate asynchronous UART reception from I²C transmission and to absorb bursts of incoming MIDI data where needed.

DC/DC Converter

We selected the TI TPS62903 integrated 3.3V DC/DC regulator used to convert the 12 V power supply voltage to 3.3 V for the MCUs. As the functional design of a DC/DC regulator was not core to the working concept of the project, we decided to simplify our design by using an integrated regulator that simply fulfilled the voltage requirements from input to output. This IC has an input voltage of up to 17 V and sustained maximum current output of 3 A, which is significantly more than the maximum current draw for 12 of the MCUs.

DSP Board

The DSP boards are on the slave side of the I2C bus of the Master Boards. These boards are paired with an electromagnetic pickup to sample a signal from a vibrating string and create feedback through an amplifier into an electromagnetic driver to continue oscillating the string.

The MCU used for these boards was the STM32L431CB as a low power microcontroller that is cheap, accessible, and hand-solderable. This allowed us to minimize both cost and power consumption in a project that utilizes several of these microcontrollers. Additionally, this MCU has an internal 16 MHz oscillator and built in DAC which reduces the overhead circuitry needed for DSP and ultimately lowers costs. As the highest harmonic we isolated was around 500 Hz, by the Nyquist sampling theorem, the sampling rate only needed to be at 2 kHz to allow for an anti-aliasing LPF at around 1 kHz. Though this MCU can process multiple concurrent audio channels, utilizing one DSP per string allowed us to avoid any bandwidth restrictions and simplify the design process by duplicating the same board layout for each string.

Pickup

The pickups were used to pick up a signal from the oscillating string, which are used to drive both the ADC for the DSP system and the master audio output.

These consist of an electromagnetic coil with an M5 steel mounting screw doubling as the core, a magnet used to magnetize the core, and turns of 28 AWG copper wire. The ferromagnetic string is magnetized by the permanent magnet at the core of the coil, and the oscillation of the string as it produces a sound induces an EMF in the coil, which becomes the signal that is amplified. Unlike the output driver, the induced EMF is difficult to estimate as the distance that the string oscillates over is hard to measure.

Utilizing a steel mounting screw that doubled as the core allowed us to save space and simplify the design by eliminating the need to add additional mounting holes to the coils, but likely contributed to a weaker pickup, as the steel screws were less ferromagnetic than anticipated and were only able to weakly magnetize the strings. This resulted in less induced EMF and a weaker signal being picked up. Most off the shelf guitar pickups use extremely thin copper wire, as it results in a higher input impedance. Since the voltage signal is the one being amplified, a higher impedance and more turns of wire result in lower current and a more sensitive pickup.

Buffer

The op-amp buffer following the pickup in the signal chain conditions the signal to appropriately drive the ADC in the MCU. Due to the high impedance of the pickup and low impedance of the MCU this is required for the ADC to ready a signal from the pickup.

Output driver

The output driver was an electromagnetic coil used to move a magnetized string and cause it to oscillate. These drivers consisted of an M5 steel mounting screw that doubled as the core, a neodymium magnet used to magnetize the core, and ~650 turns of 28 AWG copper wire. Similar to the pickup, the magnetic flux output by the coil can be approximated using Faraday's Law.

The decision to use a steel mounting screw that doubled as a core follows the same reasoning as the same decision that was made for the pickup, but likely contributed to the relatively focused magnetic flux produced by the coils due to the weak ferromagnetism of the screws. Slightly thicker wire and fewer turns were used for the output driver, resulting in a lower input impedance of 4 Ω, which allowed more current to flow through the coil and generate more magnetic flux. NEC tables do not list cable ampacities for wires under 18 AWG, so the wire thickness was selected under the assumption that it had the necessary current capability. As the selected amplifier was also optimized for delivering current to a 4 Ω speaker coil, we decided that this was an appropriate input impedance.

Amplifier

The power amplifier was used to amplify the output signal from the DSP MCU and supply sufficient current to the output coil to induce a magnetic field capable of oscillating a string. Each one was connected to the 12 V power supply that powers the entire system, allowing for higher output power than what could be supplied by an MCU or battery. We considered using a discrete class AB amplifier design, however but ultimately opted to utilize a discrete class AB amplifier IC to minimize heat dissipation.

2.2 Design details

Master Board

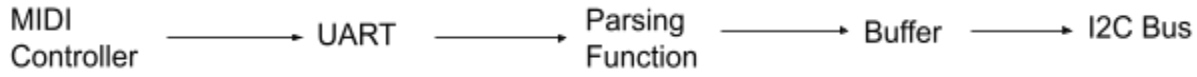

The system implements I²C communication in standard mode at 100 kHz using interrupt-driven transmission [1]. Each message packet contains a status byte and data byte which is the result of our message parsing function. Then we enqueue each packet into a circular FIFO buffer immediately upon parsing a valid MIDI command. The master initiates transmission of the oldest queued packet without blocking incoming UART signals only if the I²C bus is idle. The I²C transmit -complete interrupt advances the buffer tail upon success. At this stage, if the buffer is not empty, the interrupt handler schedules the next transmission. This buffer serves to isolate MIDI input from I²C bus timing and ensures that packets are transmitted sequentially at the maximum sustainable bus rate. When the buffer reaches capacity, the firmware discards the oldest packet to preserve real-time responsiveness, however it should be noted that this almost never happens under normal operation.

For each queued packet, the firmware computes the destination slave command directly from the MIDI note number as soon as the transmit interrupt is called. The address is calculated as:

$$Slave\ address = Base + (N \bmod 12)$$

where N is the MIDI note number and *Base* is the lowest assigned 7-bit slave address; in our system 0x10. The modulo operation maps all notes separated by octaves to the same class (0–11). This is how notes with the same pitch class route to the same slave. Notes outside the supported range are discarded before enqueueing.

If the bus returns an error, it triggers the error callback. When this happens we clear the busy state, and allow the next queued packets to resume transmission. This recovery system prevents deadlock without requiring a system reset. This was a common bug we encountered while developing with the final version of the MIDI controller.

DC/DC converter

The DC-DC converter schematic was designed from the datasheet [2] as shown in Figure 2.2.1. This circuit is able to provide 3.3 V for each of the microcontrollers, and was utilized on the master board only. The master MCU, as well as each of the DSP slave MCUs were connected in parallel to the 3.3 V (Vcc) and ground reference points of this circuit.

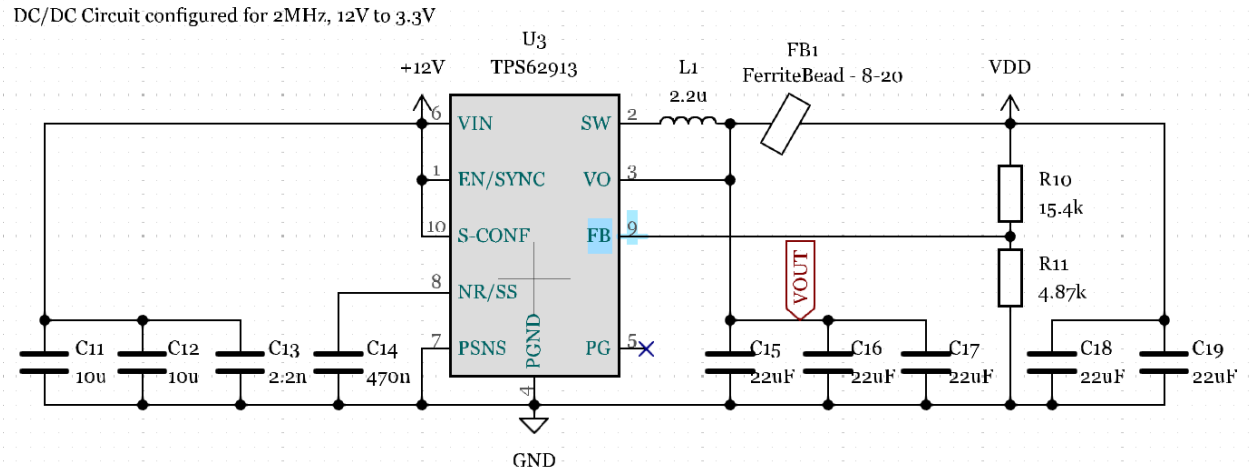

Figure 2.2.1: DC/DC converter schematic

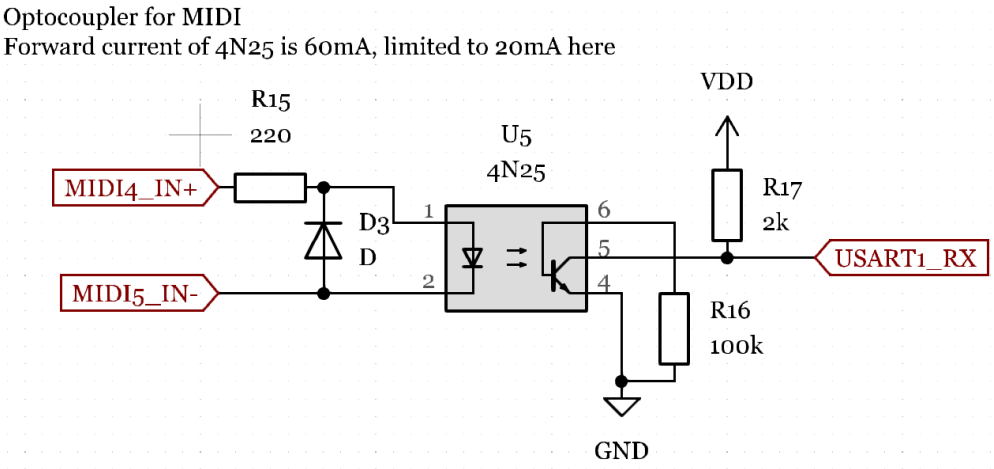

Figure 2.2.2: Optocoupler schematic

Optocoupler

The optocoupler schematic, shown in Figure 2.2.2 is a standard MIDI optocoupler circuit, limited to 20 mA at the output so as to not cause overcurrent at the UART input for the microcontroller.

DSP Board

MCU

The highest output frequency we designed around was the note B4 on the equal-tempered scale, which has a frequency of 493.88 Hz. After using a low-pass filter at 1kHz to bandlimit the output signal and prevent aliasing, the Nyquist sampling rate f_s is 2 kHz.

$$f_s = 2f$$

Our DSP process utilized an 8 kHz sample rate which was attainable from our MCU using the 4 MHz system clock with a prescaler of 4 and a counter period of 125. This sample rate limited the bandwidth through our MCU to a rate that could be accessed via DMA.

Pickup

The pickups for both master output and our DSP input were initially estimated using the values that commonly used for electric guitar pickups, roughly 1-10kΩ. Using the resistivity of copper wire $\rho = 1.68\,x\,10^{-8}\,\Omega \cdot m$ [3] and cross sectional area $A = 0.0032\,mm^2$ we can estimate that the amount of wire we would use to wind a 1 kΩ pickup would be 183 meters or in our case, approximately 6500 winds.

$$L = \frac{RA}{\rho}$$

We initially measured the output impedance of a few coils with different numbers of winds to determine the number of turns needed for our desired DC resistance. Though we anticipated a DC resistance of around 3 kΩ per coil, we determined that the pickups had comparable volume to a built-in guitar pickup at 6500 winds and only 800 Ω per coil.

Buffer

Since the typical peak-to-peak output of our pickup is around 500 mV, we decided to amplify this signal using a TL071 op-amp with a variable gain factor of up to 10. This would allow us to fully utilize our DACs reference range of 3.3 V using an input signal as small as 300 mV.

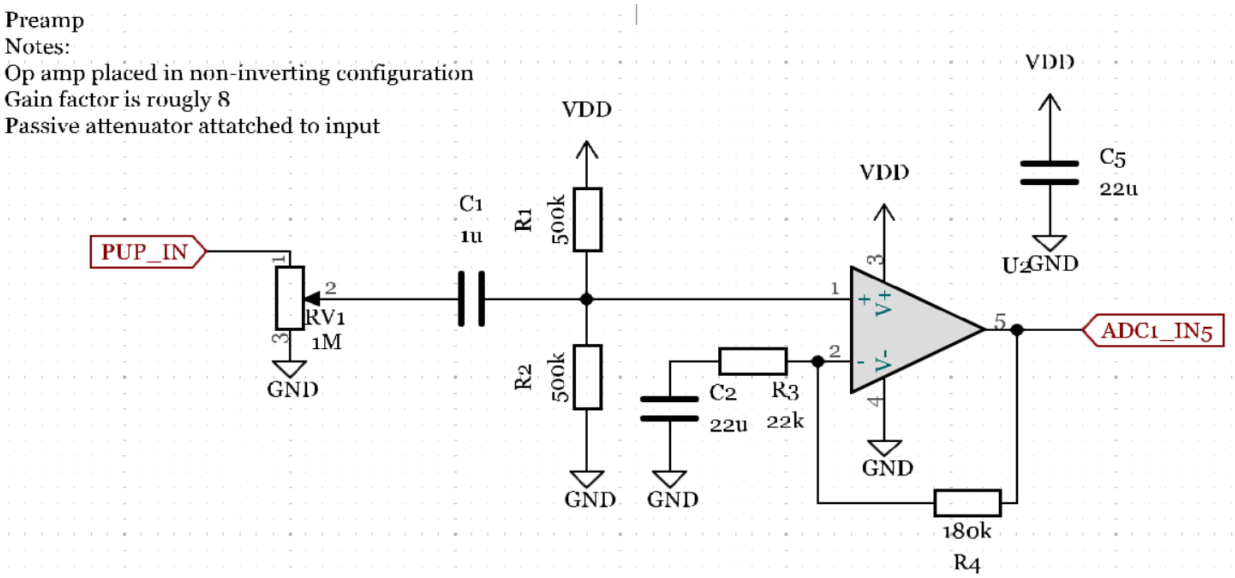

Figure 2.2.3: Buffer schematic

Additionally, a high pass filter is attached to the input of the amplifier signal in order to allow us to bias the signal to 1.65 V, allowing us to make full use of the 3.3 V range of the DAC. The DAC on our MCU has built-in analog filtering components to prevent sample aliasing, allowing us to skip this part of the circuit design.

Output driver

As each pickup consisted of copper wire wound around a plastic bobbin with an M5 screw at the core, the EMF output by each coil can be approximated using Faraday's Law.

$$\epsilon = -N(d\Phi/dt)$$

$$\Phi = B \cdot A$$

$$B = \mu_0 IN/x$$

The current in the coil is found using the output of the power amplifier and Ohm's Law. The voltage is a sine wave ranging from 0-12 V and the coil has an impedance around 4 Ω with 650 turns, resulting in a sinusoidal current signal ranging from 0-3 A. The diameter of the coil's core is estimated to be the same diameter as an M5 screw at 5 mm. As the relative permeability μ_r of carbon steel can be approximated in the order of 100 [4] and the distance from the screw head to the string was around 7 mm while the string was at rest, the induced EMF is about $0.9\ V_{rms}$.

$$B = 300 * 4\pi * 10^{-7} * 3sin(\omega t) * 650 * (1/0.007) = 105sin(\omega t)\ \text{T}$$

$$\Phi = B \cdot \pi * 0.0025^2 = 2 * 10^{-3} sin(\omega t)\ \text{Wb}$$

$$\epsilon = -1.24\omega cos(\omega t)\ \text{V}$$

Due to inefficiencies in the conversion of EMF to the actual motion of the string, as well as inefficiencies in the pickup, the actual signal level picked up was significantly less than 0.9 V.

Amplifier

As we decided to utilize the TI LM386 amplifier due to its lower power consumption and reduced heat output, we designed the amplifier circuit according to the gain 20 circuit in the datasheet [5]. The circuit is shown in Figure 2.2.4.

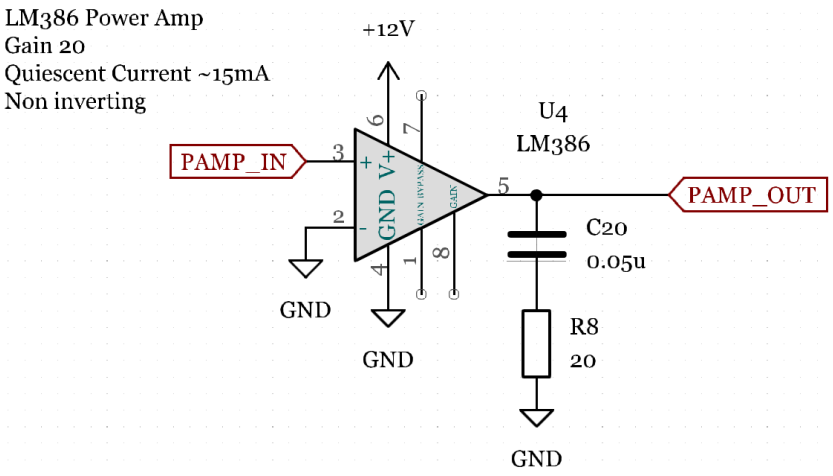

Figure 2.2.4: Power amplifier schematic

3. Verification

Master Board

Verification proceeded alongside development through the use of the Nucleo devboard and UART debug printouts. Beginning with MIDI parsing and progressing through to I²C communication while maintaining asynchronous system behavior.

Before the introduction of the real online MIDI controller, UART-based MIDI parsing was verified using a serial terminal to transmit MIDI-formatted faux hexadecimal byte sequences. When we sent Note On and Note Off messages we verified the expected debug output and onboard LED behavior, confirming correct UART RX and parsing.

Running-status behavior was validated by omitting repeated status bytes and confirming correct message reconstruction via UART debug. In addition to the standard UART debug method, I²C communication was also verified using an oscilloscope to observe waveforms as shown in Figure 3.1. The bus operated at 100 kHz with clean transitions and consistent outputs. Transmission success and failure conditions were confirmed through LED visual confirmation and error callbacks.

Asynchronous operation was validated by confirming uninterrupted MIDI byte reception during active I²C transmissions. The circular buffer handles potential backlog of MIDI messages without message loss. End-to-end latency from MIDI byte reception to I²C transmission completion was visually gauged, and proved to satisfy the expected real-time performance requirements.

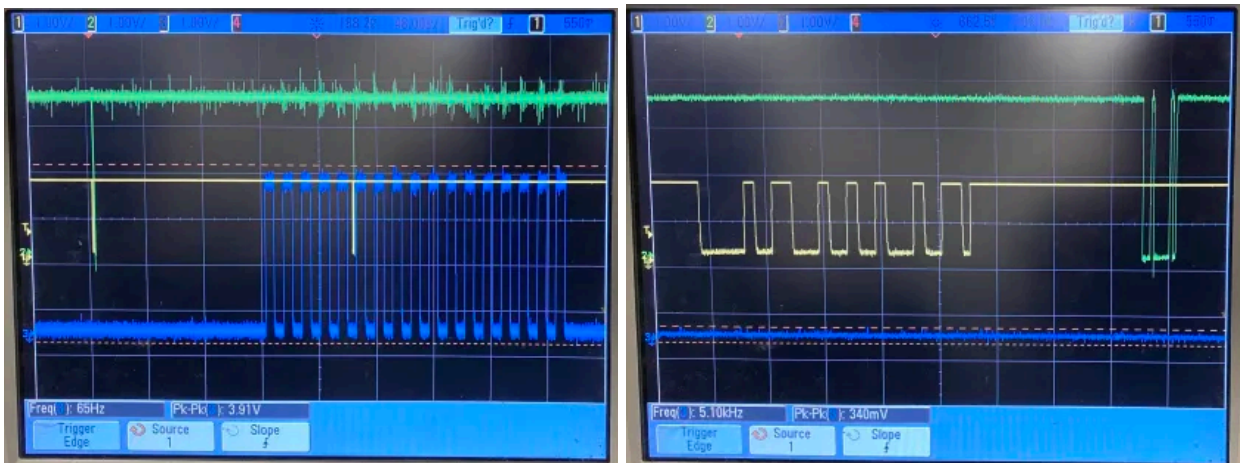

Figure 3.1 (a), (b): Scope measurement of MIDI and I2C

Power Subsystem

The sole requirement for the power subsystem was to convert the 12 V power supply voltage to 3.3 V for the microcontrollers. Verification for this subsystem could only take place after components were soldered to the PCB, as the DC/DC converter selected was a QFN package. We tested this subsystem by measuring the test points designed on the PCB for VDD (3.3 V) and ground with a multimeter and verified that the DC voltage output was 3.33 V.

DSP MCU

The primary requirements tested for the DSP MCU involved the sample rate, phase alignment, and reference voltage. As we did not connect the string feedback system to the DSP boards, only the output signal was measured in an oscilloscope. The DSP MCU was able to output a signal at 493 Hz without aliasing. Figure 3.2 shows the DSP outputting a C2 (65 Hz). Though there was some frequency inaccuracy (5-9 Hz)in the output at higher frequencies, we were able to adjust for this by carefully tuning strings until we could hear them resonating. In Figure 3.2, it is also apparent that the output voltage is centered around 1.75 V, which is 0.1 V off of Vcc/2.

Pickups

Our pickups ultimately wound up with 6500 turns. After measuring the terminals with a multimeter, we determined that this resulted in a lower DC resistance than planned at 800 Ω rather than 3 $k\Omega$.

Though we did not verify the peak to peak voltage of the pickups using an oscilloscope, we were able to determine that the pickups had comparable volume to a built-in guitar pickup when the string was plucked by connecting both the guitar and the pickups to a guitar amplifier. Consequently, we concluded that the lower output impedance was still acceptable based on the final output signal level.

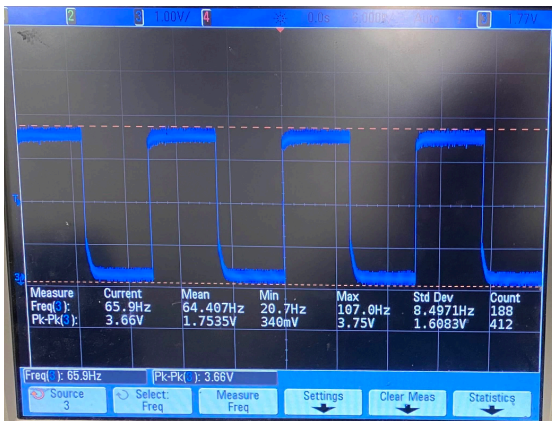

Figure 3.2: DSP output playing a C2 (65Hz)

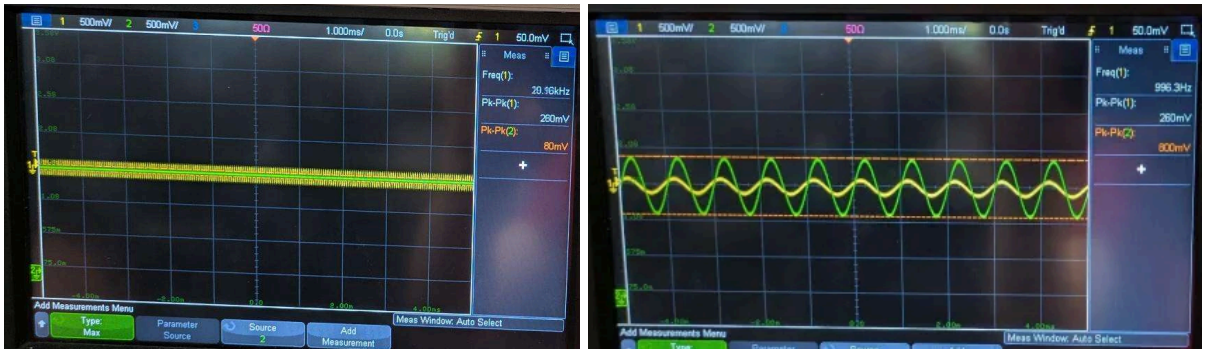

Figure 3.3 (a), (b): Buffer bandlimit and gain

Buffer

We were able to test and verify each of the requirements for the buffer by probing the output with an oscilloscope and supplying an input signal with a function generator. Figure 3.3 (a) shows the buffer band limit at 20 kHz and (b) shows a gain factor of 3 at nearly 1 kHz.

Output Driver

Our output drivers utilized 650 turns of wire, and we measured 4.5 Ω across the terminals of the coil using a multimeter. Though this is lower than the $6 - 8\ \Omega$ range we initially designed for, this was a consideration made to avoid excessive heating in the coil and the power amplifier. As there was no damage to either, we determined that the 4.5 Ω impedance was acceptable.

The maximum ampacity of the coil was not tested, as this would require destructive testing which we felt was unnecessary as long as the coil could withstand the anticipated current of 500 mA. As the coils did not heat up substantially under continuous operation, we concluded that they could withstand the necessary current.

Power Amplifier

Though we did not measure the input impedance of the power amplifier, the fact that the device was able to operate with a continuous note on signal for 1 minute when tested indicated that the input current was sufficiently low to avoid damaging the device. Measuring the output of the amplifier with an oscilloscope revealed that the gain factor was sufficient for the output voltage to utilize the full 12 V range of the supply voltage while the output of the amplifier was connected to a 4 Ω load, indicating it was able to supply the maximum possible current to the output coil.

4. Costs

Estimating the total cost of this project involves summing the total value of the bill of materials (Table 4.1) with the labor cost estimate for each partner and for the machine shop hours. The sum of the items on the bill of materials is $122.50.

For each partner, the labor cost estimate uses the following formula:

$$salary * hours * 2.5$$

Only including hours spent on assembly, this totals to around $7,500. Adding on an aggressive estimate of the machine shop hours spent adds around $2,000 to the final cost. Including design hours, this adds about another $15,000 to the cost, but this also includes time spent researching for each partner, and would not accurately represent the manufacturing cost.

All in all, the estimated cost of this project was $9622.50, which is not economically feasible even for a novel synthesizer. Though this is likely manufacturable at scale which would reduce costs, the assembly of 12 PCBs, in addition to the coils and the backing board still take substantial labor hours.

Component	component price	supplier	manufacturer	manufacturer pn	quantity
4N25 Optocoupler	$0.67	Mouser	Vishay	4N25	1
Buck Converter	$2.40	Mouser	TI	TPS62913RPUR	1
MCU	$3.02	Mouser	STM	STM32L431CBT6	12
TL071 Op Amp	$0.17	Mouser	TI	TL071HIDCKR	12
2.2 uH inductor	$1.93	Mouser	Wurth	74438356022	1
DC Barrel Jack	$1.40	Mouser	Same Sky	PJ-063AH	1
2.2nF 0402	$0.10	Mouser	Murata	GRM155R71H222JA01J	1
470nF 0402	$0.31	Mouser	AVX	04023D474KAT2A	1
4.87 kΩ 0402	$0.16	Mouser	Vishay	MCS04020C4871FE0000	1
15.4 kΩ 0402	$0.23	Mouser	Vishay	TNPW040215K4BEED	1
10uF 0805	$0.11	Mouser	Samsung	CL31A106KBHNNNE	2
Ferrite Bead	$0.10	Mouser	TDK	MPZ1005S100CT000	1
22 uF 0805	$0.10	Mouser	Samsung	CL21A226MAYNNNE	29
1 MΩ 0805	$0.10	Mouser	Vishay	CRCW08051M00FKEA	24
22 kΩ 0805	$0.02	Mouser	Bourns	CR0805-JW-223ELF	36

180 kΩ 0805	$0.02	Mouser	Bourns	CR0805-JW-184ELF	12
4.7 nF 0805	$0.08	DigiKey	Samsung	CL21B472KDCNNNC	12
1 uF 0805	$0.01	DigiKey	Samsung	CL21B105KBFNNNE	24
LM386 Op Amp	$0.68	DigiKey	TI	LM386N-3/NOPB	12
20 Ω 0805	$0.05	DigiKey	Panasonic	ERJ-P06J100V	12
47 nF 0805	$0.05	DigiKey	Wurth	885012207096	12
Schottky Diode	$0.34	Mouser	AVX	SD0805S020S1R0	1
12V 5A Power Supply	$9.89	Amazon			1
Tuning Mechanisms	$15.69	Amazon			2
M5 Wood Inserts	$12.79	Amazon			1
0.1 uF 0805	$0.10	Mouser	Samsung	CL21B104MACNNNC	48
100 kΩ 0805	$0.03	DigiKey	Yageo	RC0805FR-07100KL	14
220 Ω 0805	$0.10	Mouser	Susumu	RG201P-221-B-T5	1
2 kΩ 0805	$0.12	Mouser	Vishay	TNPW08052K00FEEA	1

Table 4.1: Bill of Materials

5. Conclusions

Our goal with this project was to build a MIDI-controlled synthesizer with harmonic control that utilizes 12 oscillating strings driven by electromagnetic coils to play different notes. Similar to a guitar, these strings oscillate over a magnetic pickup and induce an EMF which is then amplified in an amplifier.

Our final design demonstrates working UART-based MIDI parsing of different note on and note off signals. Using I2C communication, this was able to control the frequency of a note output by the DSP. This signal was then successfully amplified through the power amplifier and used to drive the output driver coil to oscillate a string. Though the pickups and driver coils of our final design had inefficiencies that resulted in the output signal being inaudible over the pickups, we were able to demonstrate the functionality of our signal chain with a prototype coil using a different core material and a guitar with pickups that are better optimized for picking up small signals produced by the oscillating strings.

Given more time, we would be able to alter our design so that the pickups and driver coils were more powerful and were better able to drive the guitar string and pick up the signal. In terms of design, this would likely mean changing the core material and gluing down the magnets used to magnetize the cores more strongly so that there is less EMF lost to the magnets and cores vibrating rather than the strings.

In a broader context, this project demonstrates nuances of speaker coil and amplifier design, particularly in sources of loss but also demonstrates a unique instrument scheme and timbre for a synthesizer, allowing for new potential musical sounds.

In adhering to the IEEE Code of Ethics [6], we have prioritized the safety, health, and welfare of the public in utilizing lead-free components where possible, as well as optimizing power consumption and minimizing heat output of our system that is mounted to a wood surface to avoid possible fire hazards. We have accepted criticism of our technical work and acknowledged and corrected errors in our designs. We have been honest and realistic in our claims and estimates based on our available data, and we have appropriately credited the contributions of others.

6. References

[1] *STM32L431xx*, datasheet, STMicroelectronics, 2018. Available at: https://www.st.com/content/ccc/resource/technical/document/datasheet/group3/83/b3/60/f6/b1/cc/47/7e/DM00257211/files/DM00257211.pdf/jcr:content/translations/en.DM00257211.pdf

[2] *TPS62913*, datasheet, Texas Instruments, 2021. Available at: https://www.ti.com/lit/ds/symlink/tps62913.pdf?ts=1765353607151&ref_url=https%253A%252F%252Fwww.ti.com.cn%252Fproduct%252Fcn%252FTPS62913

[3] R. A. Matula, "Electrical resistivity of copper, gold, palladium, and silver," in *Journal of Physical and Chemical Reference Data*, 1979, pp. 1147

[4] S. W. Ellingson, “Permeability of Some Common Materials,” Virginia Tech Libraries' Open Education Initiative

[5] *LM386 Low Voltage Audio Power Amplifier*, datasheet, Texas Instruments, 2023. Available at: https://www.ti.com/lit/ds/symlink/lm386.pdf?ts=1734118207298

[6] Institute of Electrical and Electronics Engineers, ‘IEEE Code of Ethics’, June 2020. [Online]. Available: https://www.ieee.org/about/corporate/governance/p7-8